Interconversion of $FeC_2H_3^+$ and $HFeC_2H_2^+$: An FTICR and Density Functional Study

Huiping Chen,* Denley B. Jacobson,† and Ben S. Freiser‡

H. C. Brown Laboratory of Chemistry, Purdue University, West Lafayette, Indiana 47907

Received April 23, 1999

The geometries and energetics of four $FeC_2H_3^+$ isomers ($Fe(CHCH_2)^+$ (**1**), $HFe(CHCH)^+$ (**2**), $(H)_2Fe(CCH)^+$ (**3**), and $HFe(CCH_2)^+$ (**4**)) have been studied by a hybrid of density functional theory (DFT) and the Hartree−Fock approach (BECKE3LYP). **1** ($^5A''$) is the global minimum on the quintet surface with **2** ($^5A''$) 18.5 kcal/mol higher in energy. The activation barrier for **1** → **2** conversion is 36.8 kcal/mol with respect to **1** ($^5A''$). On the triplet surface, **1** ($^3A''$) is also the global minimum with **2** ($^3A''$) 9.1 kcal/mol higher, and the activation barrier from **1** to **2** is only 12.1 kcal/mol. The bond dissociation energy $D°(FeH^+-C_2H_2)$ for the quintet ground state is predicted to be 32.9 kcal/mol, which compares well with the experimentally measured $D°(Fe^+-C_2H_2)$ value of 32 kcal/mol. The [Fe, C_2, H_3]$^+$ system is also studied experimentally by using Fourier transform ion cyclotron resonance mass spectrometry (FTICR-MS). *In situ* synthesis of $FeC_2H_3^+$ is achieved by a complex, multistep procedure involving ion/molecule reactions in conjunction with CID and SORI-CID techniques. CID and SORI-CID of $FeC_2H_2D^+$ give competitive losses of C_2HD and C_2H_2 to yield FeH^+ and FeD^+. Moreover, FeH^+/FeD^+ react with C_2D_2/C_2H_2 to yield rapid H/D exchange, forming FeD^+/FeH^+. These results suggest that interconversion between **1** and **2** is facile for activated **1** and **2** as predicted by theory. Reaction of $FeC_2H_3^+$ with C_2H_2 yields exclusive formation of FeC_2H^+. The collision complex, $FeC_4H_5^+$, further reacts with C_2H_2 to yield benzene loss. Kinetics for H/D exchange reactions between FeH^+/FeD^+ and C_2D_4/C_2H_4 are also measured and provide complementary information to Schwarz's studies of the [Fe, C_2, H_5]$^+$ system.

Introduction

The process in which an unsaturated organic ligand (alkene, alkyne, etc.) formally inserts into an adjacent bond is called migratory insertion[1,2] and is ubiquitous in organo-transition-metal chemistry. Migratory insertions are generally reversible and proceed with retention of stereochemistry of the migrating group. The general process for alkene and alkyne insertion (reaction 1)

(1)

involves migration of a proximal *cis*-alkyl or *cis*-hydride ligand to the unsaturated group on the metal. This is the key step in homogeneous hydrogenation and in many alkene and alkyne alkylation procedures.[2−4] The reverse of alkene/alkyne insertion into a metal hydride is β-hydride elimination, a process which often compromises the stability of σ-hydrocarbyl−transition-metal complexes. The corresponding β-alkyl eliminations are rarely observed.

Facile, reversible β-hydride elimination/insertion reactions have frequently been invoked in transition-metal gas-phase ion chemistry.[5−8] However, there have been few systematic studies regarding this process in the gas phase. Recently, Schwarz and co-workers presented a detailed study on the interconversion of $Fe(CH_2CH_3)^+$ with $HFe(CH_2CH_2)^+$ (reaction 2) by both theory and

$$HFe(CH_2CH_2)^+ \rightleftharpoons Fe(CH_2CH_3)^+ \qquad (2)$$

experiment.[9] Theory predicts that quintet $Fe(CH_2CH_3)^+$ ($^5A'$) is the global minimum with $HFe(CH_2CH_2)^+$ ($^5A'$) being 13 kcal/mol less stable. There is a significant barrier (36 kcal/mol) for their interconversion by β-hydride transfer. The triplet surface was also studied where $Fe(CH_2CH_3)^+$ ($^3A''$) and $HFe(CH_2CH_2)^+$ ($^3A''$) were found to lie 14 and 27 kcal/mol, respectively, above $Fe(CH_2CH_3)^+$ ($^5A'$). The barrier for the interconversion along the triplet surface is 8 kcal/mol below that of the

* To whom correspondence should be addressed. Present address: Wyeth-Ayerst Research, Building 222/1044, 401 N. Middletown Road, Pearl River, NY 10965.
†Department of Chemistry, North Dakota State University, Fargo, ND 58104.
‡ Deceased on December 31, 1997.

(1) Pruchnik, F. P. *Organometallic Chemistry of the Transition Elements*; Plenum Press: New York and London, 1990.
(2) Swan, J. M.; Black, D. St. C. *Organometallics in Organic Synthesis*; Chapman and Hall: London, 1974.
(3) Topchiev, A. V.; Zavgorodnii, S. V.; Kryuchkova, V. G. *Alkylation with Olefins*; Elsevier: Amsterdam, London, New York, 1964.
(4) Collman, J. P.; Hegedus, L. S.; Norton, J. R.; Finke, R. G. *Principles and Applications of Organotransition Metal Chemistry*; University Science Books: Mill Valley, CA, 1987.
(5) Eller, K.; Schwarz, H. *Chem. Rev.* **1991**, *91*, 1121.
(6) van Koppen, P. A. M.; Brodbelt-Lustig, J.; Bowers, M. T.; Dearden, D. V.; Beauchamp, J. L.; Fisher, E. R.; Armentrout, P. B. *J. Am. Chem. Soc.* **1991**, *113*, 2359.
(7) Fiedler, A.; Schröder, D.; Schwarz, H.; Tjelta, B. L.; Armentrout, P. B. *J. Am. Chem. Soc.* **1996**, *118*, 5047.
(8) Czekay, G.; Drewello, T.; Schwarz, H. *Organometallics* **1989**, *8*, 4561.
(9) Fiedler, A.; Schröder, D.; Zummack, W.; Schwarz, H. *Inorg. Chim. Acta* **1997**, *259*, 227.

10.1021/om9902941 CCC: $18.00
Publication on Web 11/30/1999

corresponding quintet surface. This lower barrier suggests that the triplet surface may play an important role in this interconversion.

Related to the above process is the interconversion between transition-metal ethenyl complexes and hydrido−ethyne complexes (reaction 3). Schaefer and co-

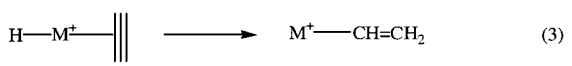

(3)

workers studied H−Al−C_2H_2 by theory.[10] The Al−C_2H_2 complex has been observed by ESR, IR, and UV spectroscopy and is clearly an open-shell radical, leading to the possibility that hydrogenated Al−C_2H_2 might be stable. Among the three reasonable isomers, the ethenyl−Al structure is calculated to be the most stable. In addition, metal−vinylidene complexes (M=C=CRR′; R, R′ = H, CH_3, CF_3, and many other types of substituents) are of current interest and can be reversibly converted to vinyl complexes, by either protonation or alkylation.[11] Recent studies on the ethenyl complex (μ-H)$Os_3(CO)_9(PPh_3)(\mu$-CH=CH_2) have demonstrated the presence of two isomers which can be interconverted through the fluxional behavior of the bridging vinyl group.[12,13]

The structures and reactivities of $MC_2H_3^+$ ions have not yet been extensively investigated in the gas phase. Armentrout and co-workers,[14−16] using ion beam techniques, measured the following bond dissociation energies: $D°(Co^+-C_2H_3)$ = 48.4 ± 1.8 kcal/mol, $D°(Cr^+-C_2H_3)$ = 54.1 ± 1.4 kcal/mol, $D°(Fe^+-C_2H_3)$ = 56.8 ± 2.5 kcal/mol, $D°(Ti^+-C_2H_3)$ = 79.9 ± 5.8 kcal/mol, and $D°(V^+-C_2H_3)$ = 88.1 ± 4.6 kcal/mol. $MC_2H_3^+$ ions (M = transition metals) are difficult to study because there is no direct means to their generation. As a complement to Schwarz's study on the [Fe, C_2, H_5]$^+$ system we have studied the [Fe, C_2, H_3]$^+$ system. Here, the in situ synthesis of [Fe, C_2, H_3]$^+$ is described and the results of experimental studies by using Fourier transform ion cyclotron resonance (FTICR) mass spectrometry are presented. We also performed a comprehensive theoretical investigation of different [Fe, C_2, H_3]$^+$ isomers ($Fe(CHCH_2)^+$ (**1**), $HFe(CHCH)^+$ (**2**), $(H)_2Fe(CCH)^+$ (**3**), and $HFe(CCH_2)^+$ (**4**)) in which the minima and the saddle points on the [Fe, C_2, H_3]$^+$ potential energy surface (PES) are obtained by using density functional theory (DFT).[17,18]

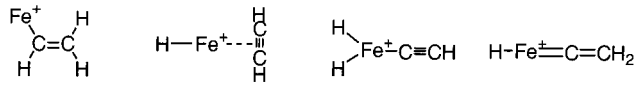

1 **2** **3** **4**

Experimental Section

All experiments were performed by using a Nicolet (now Finnigan FT/MS, Madison, WI) FTMS-2000 Fourier transform ion cyclotron resonance (FT-ICR) mass spectrometer equipped with a dual trapping cell in a 3 T magnetic field. A complete description of the instrument is given elsewhere.[19]

Chemicals were obtained commercially in high purity and were used as supplied, except for multiple freeze−pump−thaw cycles to remove noncondensable gases from liquids. Methane was introduced into the vacuum chamber via a Varian leak valve at a static background pressure of ~3.3×10^{-6} Torr as the reagent gas for chemical ionization and as the collision gas for collision-induced dissociation (CID)[20] and sustained off-resonance irradiation (SORI) CID experiments.[21] The maximum translational energy E_{tr}(max) acquired during CID by the ions is given in the laboratory frame and was calculated by using the following equation applicable to a cubic cell:

$$E_{tr}(\max) = \frac{E^2 q^2 t^2}{16 M_{ion}}$$

where E is the electric field amplitude, t is the duration of the applied electric field, q is the ion charge, and M_{ion} is the mass of the irradiated ion.[22,23] CID fragment ion intensities are plotted as a fraction of the total ion intensity at each kinetic energy. The duration of the excitation pulse is 500 μs, with the electric field amplitude varied to control ion kinetic energy. A 50 ms delay follows ion irradiation to allow for ion collisions and decomposition prior to subsequent isolation or detection.

In addition to conventional FTICR-CID, CID by using sustained "off-resonance" irradiation (SORI)[21] for ion activation was also employed to determine the lowest energy fragmentation pathways. For SORI-CID, ions are irradiated "off-resonance" for 500 ms. The *maximum* ion kinetic energy is calculated by using the equation

$$E_{tr}(\max) = \frac{E^2 q^2}{2 M_{ion}(\omega_1 - \omega_c)^2}$$

where ω_1 (rad s^{-1}) is the excitation frequency and ω_c is the natural cyclotron frequency of the ion.

For kinetic studies, neutral reagents were introduced into the vacuum chamber through Varian leak valves. The pressure of neutrals was measured by using an ion gauge that was calibrated to determine the pressure gradient between the reaction cell and ion gauge. Finally, the pressure was corrected for ionization sensitivities. The uncertainty in the absolute pressure of neutral reagents is less than ±30%. The uncertainty in pressure is the largest contributor to errors in reaction rate constants. Consequently, we assign an absolute error of ±30% for reaction rate constants, while the relative reaction rate constants are more reliable.

Computational Details

Calculations were performed with the Gaussian 94/DFT program package[24] at the Purdue University Computer Center (PUCC) and on a Silicon Graphics O2 workstation in our laboratory. For the computational studies, a hybrid of DFT and Hartree−Fock (HF) was applied in which the Becke-3-LYP functional[25−28] was first combined with the standard effective core potential for Fe^+ and the Dunning−Hay double-ξ

(10) Xie, Y.; Schaefer, H. F., III. *J. Am. Chem. Soc.* **1990**, *112*, 5393.
(11) Wang, L. S.; Cowie, M. *Organometallics* **1995**, *14*, 2374.
(12) Koike, M.; Hamilton, D. H.; Wilson, S. R.; Shapley, J. R. *Organometallics* **1996**, *15*, 4930.
(13) Shapley, J. R.; Richter, S. I.; Tachikawa, M.; Keister, J. B. *J. Organomet. Chem.* **1975**, *94*, C43.
(14) Aristov, N.; Armentrout, P. B. *J. Am. Chem. Soc.* **1986**, *108*, 1806.
(15) Fisher, E. R.; Armentrout, P. B. *J. Am. Chem. Soc.* **1992**, *114*, 2039.
(16) Schultz, R. H.; Armentrout, P. B. *Organometallics* **1992**, *11*, 828.
(17) Labanowski, J. K.; Andzelm, J. W. *Density Functional Methods in Chemistry*; Springer-Verlag: New York, 1991.
(18) Laird, B. B., Ross, R. B., Ziegler, T., Eds. In *Chemical Applications of Density-Functional Theory;* ACS Symposium Series 629; American Chemical Society: Washington, DC, 1996.
(19) Gord, J. R.; Freiser, B. S. *Anal. Chim. Acta* **1989**, *225*, 11.
(20) Freiser, B. S. *Talanta* **1985**, *32*, 697.
(21) Gauthier, J. W.; Trautman, T. R.; Jacobson, D. B. *Anal. Chim. Acta* **1991**, *246*, 211.
(22) Grosshans, P. B.; Marshall, A. G. *Anal. Chem.* **1991**, *63*, 2057.
(23) Freiser, B. S. *Techniques for the Study of Ion Molecule Reactions*; Farrar, J. M., Saunders,: W. H., Jr., Eds.; Wiley: New York, 1988; p 61.

basis set for C and H atoms. The calculations were then repeated with the cc-pVTZ[29] basis set for C and H. For iron, the (14s9p5d) primitive set of Wachters[30] supplemented with one diffuse p function, one diffuse d function, and one diffuse f function according to Bauschlicher[31] is used, resulting in a (62111111|331211|3111|3) → [8s6p4d1f] contraction. The ground state of Fe^+ is considered as ^6D ($3d^64s^1$), even though the Becke-3-LYP scheme incorrectly predicts ^4F as the ground state, due to the bias in DFT for d^n over $d^{n-1}s^1$ configurations.[32] The DFT/HF hybrid method has been found to yield molecular geometries that are qualitatively comparable with those obtained at highly correlated levels. Although the computed thermochemistry is reasonable, bond dissociation energies (BDEs) tend to be slightly overestimated. Therefore, the accuracy of the DFT/HF approach for transition-metal compounds is estimated to be within ±10 kcal mol^{-1} for BDEs and ±5 kcal mol^{-1} for the relative energies of isomeric $FeC_2H_3^+$ species. All stationary points were characterized as minima or first-order transition structures by evaluating the frequencies and normal modes by using analytical first derivatives and the computed force constant matrix. Corrections for zero point energies have been taken into account, and different spin configurations have been considered for Fe^+.

Results and Discussion

Computational Studies. 1. $Fe(CHCH_2)^+$. Among the four reasonable isomers, we first consider the $Fe(CHCH_2)^+$ structure, **1**, where a vinyl group is bound to the metal ion as an intact ligand. The initial interaction could occur as Fe^+ (^6D) and $C_2H_3^\bullet$ approach each other to form an iron−vinyl ion complex. The optimized geometries of **1** ($^5A''$) and **1** ($^3A''$) are shown in Figure 1. The ground state, **1** ($^5A''$) has C_1 symmetry with a short, covalent Fe−C bond (1.923 Å). Mulliken population analysis gives the charge distribution as follows: $q = +0.852$ for Fe and $q = +0.148$ for the C_2H_3 group, consistent with covalent bonding. The vinyl unit in the complex is only slightly distorted from that of a free $C_2H_3^\bullet$ radical.[33] The C−C bond is elongated from 1.301 to 1.331 Å, indicating the formation of an Fe−C bond that apparently weakens the original C−C double bond. Bonding of the vinyl group to Fe^+ results in a decreased C−C−H_3 bond angle (from 138.6° for free C_2H_3 to 123.5°). Hence, the bond angles for **1** closely resemble that for ethene, consistent with covalent bonding between the metal and vinyl group. The other C−H bond lengths and C−C−H bond angles only exhibit slight changes over free C_2H_3, as shown in Figure 1. These

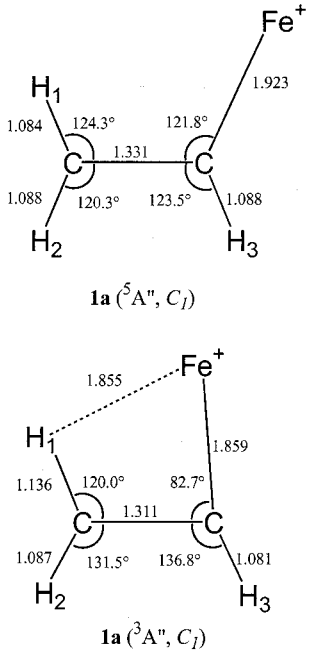

Figure 1. Optimized geometries of the quintet and triplet states of $Fe(CHCH_2)^+$ (bond lengths in Å and bond angles in deg).

results suggest that the iron vinyl cation is formed by spin pairing of ground-state Fe^+ (^6D) and doublet $C_2H_3^\bullet$ ($^2A'$), giving rise to a quintet ground state. The dissociation energy to form Fe^+ (^6D) and doublet $C_2H_3^\bullet$ ($^2A'$) from **1** ($^5A''$) is predicted to be 71.7 kcal/mol with ZPVE corrections, compared with the experimental value of 56.8 ± 2.5 kcal/mol previously reported by Armentrout and co-workers.[16] As is well-known, the Becke-3-LYP approach has a slight energetic preference for low-spin configurations. Therefore, the bond dissociation energy (BDE) is overestimated due to overestimation of the energy for ground-state Fe^+ (^6D, $3d^64s^1$).

The corresponding $^3A''$ state of **1** is predicted to be 17.9 kcal/mol less stable than the quintet state. Optimization of the structure of **1** ($^3A''$) features some dramatic differences from that for the quintet state (Figure 1). First of all, a much smaller Fe−C−C bond angle of 82.7° is observed. The Fe−C bond length is decreased to 1.859 Å. In comparison to structure **1** ($^5A''$), the C−H_1 bond is significantly increased from 1.084 to 1.136 Å and the C−C bond is shortened by 0.02 Å. The contraction of the Fe−C−C bond angle and the elongation of the C−H_1 bond suggests an agostic interaction with Fe. Schwarz and co-workers reported a similar finding for the triplet state of $Fe(CH_2CH_3)^+$.[9] In our case, the in-plane Fe−H distance is 1.855 Å, as compared to 1.75 Å in their system. Although the structural features for the triplet state are consistent with agostic interactions, it is obvious that this type of interaction is not operative for the ground state of the high-spin system.

2. $HFe(CHCH)^+$. The optimized geometry of $HFe(CHCH)^+$, **2** ($^5A''$), is shown in Figure 2 and has C_s symmetry. A covalent Fe−H bond (1.575 Å) is observed, and Fe is 2.306 Å above the middle point of the C_2H_2 unit. Mulliken population analysis yields the following charge distributions: $q = +0.654$ for FeH and $q = +0.346$ for the C_2H_2 group. The C−C bond length (1.208 Å) of the acetylene unit in the complex resembles that

(24) Frisch, M. J.; Trucks, G. W.; Schlegel, H. B.; Gill, P. M. W.; Johnson, B. G.; Robb, M. A.; Cheeseman, J. R.; Keith, T.; Petersson, G. A.; Montgomery, J. A.; Raghavachari, K.; Al-Laham, M. A.; Zakrzewski, V. G.; Ortiz, J. V.; Foresman, J. B.; Peng, C. Y.; Ayala, P. Y.; Chen, W.; Wong, M. W.; Andres, J. L.; Replogle, E. S.; Gomperts, R.; Martin, R. L.; Fox, D. J.; Binkley, J. S.; Defrees, D. J.; Baker, J.; Stewart, J. P.; Head-Gordon, M.; Gonzalez, C.; Pople, J. A. Gaussian 94, Revision D.1; Gaussian, Inc., Pittsburgh, PA, 1995.
(25) Becke, A. D. *Phys. Rev.* **1988**, *A38*, 3098.
(26) Becke, A. D. *J. Chem. Phys.* **1993**, *98*, 1372.
(27) Becke, A. D. *J. Chem. Phys.* **1993**, *98*, 5648.
(28) Stephens, P. J.; Devlin, F. J.; Chabalowski, C. F.; Frisch, M. *J. Phys. Chem.* **1994**, *98*, 11623.
(29) Dunning, T. H., Jr. *J. Chem. Phys.* **1989**, *90*, 1007.
(30) Wachters, A. J. H. *J. Chem. Phys.* **1970**, *52*, 1033.
(31) Bauschlicher, C. W.; Langhoff, S. R., Jr.; Barnes, L. A. *J. Chem. Phys.* **1989**, *91*, 2399.
(32) Ziegler, T.; Li, J. *Can. J. Chem.* **1994**, *72*, 783.
(33) Geometry of ground-state free C_2H_3 radical with Becke3LYP/cc-PVTZ: R(C1−C2) = 1.301 Å, R(H1−C1) = 1.086 Å, R(H2−C1) = 1.091 Å, R(H3−C2) = 1.078 Å, ∠H1−C1−C2 = 122.3°, ∠H2−C1−C2 = 121.9°, ∠H3−C2−C1 = 138.6°.

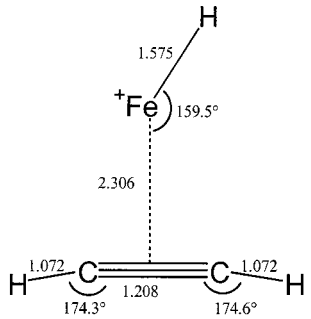

2a (^{5}A", C_s)

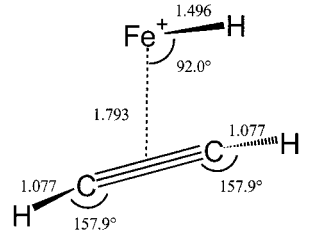

2a (^{3}A", C_1)

Figure 2. Optimized geometries of the quintet and triplet states of $HFe(CHCH)^+$ (bond lengths in Å and bond angles in deg).

for free acetylene (1.20 Å).[34] The C−H bonds are slightly bent away from the FeH^+ unit, as is typically observed for transition-metal−acetylene complexes.[35,36] The bare iron hydride cation, FeH^+, has a $^5\Delta$ ground state. Therefore, **2** (^{5}A″) on the quintet surface can simply arise from complexation of acetylene to FeH^+, which is consistent with the structural features observed. $D°(FeH^+-(CHCH))$ is calculated to be 32.9 kcal/mol with ZPVE correction and compares well with $D°(Fe^+-(CHCH)) = 32$ kcal/mol.[37] This result suggests a similar bonding nature in $Fe(CHCH)^+$ and $HFe(CHCH)^+$ complexes.

The corresponding triplet species **2** (^{3}A″) is less stable by 8.5 kcal/mol than **2** (^{5}A″). It has C_1 symmetry and displays some structural differences compared to **2** (^{5}A″). For example, the Fe−H bond is completely out of the Fe−C−C plane, by almost 92.0°. In addition, the Fe−H bond is shorter (1.496 Å) and Fe is closer to the acetylene unit (1.793 Å above). These dramatic changes may essentially favor the donation/back-donation bonding interaction between FeH^+ and C_2H_2 of the triplet state. Similar findings were also reported in Schwarz's work.[9]

3. Transition State between $Fe(CHCH_2)^+$ and $HFe(CHCH)^+$. The saddle point $TS_{1/2}$ for interconversion of **1** and **2** on both the quintet and triplet PES's have similar structures with C_1 symmetry but with somewhat different bond lengths and bond angles (Figure 3). $TS_{1/2}$ (^{5}A″) is located 36.8 kcal/mol above **1** (^{5}A″) and is characterized by an imaginary frequency,

(34) Geometry of free acetylene with Becke3LYP/cc-PVTZ: R(C−C) = 1.196 Å.
(35) Sodupe, M.; Bauschlicher, C. W. *J. Phys. Chem.* **1991**, *95*, 8640.
(36) Hoffman, D. M.; Hoffman, R.; Fisel, C. R. *J. Am. Chem. Soc.* **1982**, *104*, 3858.
(37) MacMahon, T. J.; Jackson, T. C.; Freiser, B. S. *J. Am. Chem. Soc.* **1989**, *111*, 421.

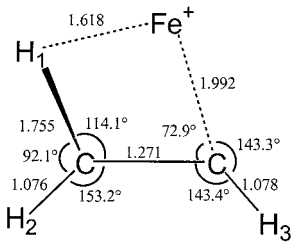

$TS_{1a/2a}$ (^{5}A", C_1)

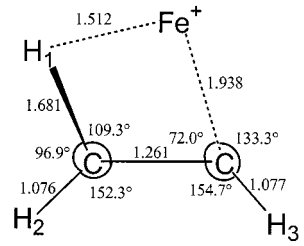

$TS_{1a/2a}$ (^{3}A", C_1)

Figure 3. Optimized geometries of the quintet and triplet states of $TS_{1/2}$ (bond lengths in Å and bond angles in deg).

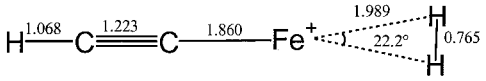

3a (^{5}A", C_1)

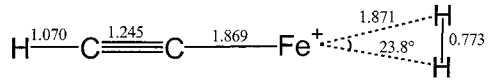

3a (^{3}A", C_s)

Figure 4. Optimized geometries of the quintet and triplet states of $(H)_2Fe(CCH)^+$ (bond lengths in Å and bond angles in deg).

1012.5i cm^{-1}, which corresponds to the β-H migration involving the metal center. The C−C bond length is 1.271 Å, which falls between the lengths of double and triple carbon−carbon bonds. In comparison to the structure of **1** (^{5}A″), the Fe−C bond length is elongated by 0.067 Å. The $C-H_1$ bond length increases significantly from 1.084 to 1.755 Å. In addition, the Fe−C bond is bending toward the elongated $C-H_1$ bond, resulting in a reduced Fe−C−C bond angle of 72.9°.

The optimized geometry of $TS_{1/2}$ (^{3}A″) resembles that on the quintet surface. This transition state is characterized by an imaginary frequency of 668.9i cm^{-1}. Surprisingly, it is found to be 6.8 kcal/mol more stable than $TS_{1/2}$ (^{5}A″). Schwarz and co-workers also found a similar crossing of the triplet and quintet PES for the $[Fe, C_2, H_5]^+$ system.[9] On the basis of the curve crossing in the TS region, they concluded that the interconversion of $Fe(CH_2CH_3)^+$ and $HFe(CH_2CH_2)^+$ may proceed by passage via the energetically less demanding low-spin surface connecting the two isomers. This curve crossing is also possible for our $[Fe, C_2, H_3]^+$ system.

4. $(H)_2Fe(CCH)^+$. $(H)_2Fe(CCH)^+$, **3**, can be generated by insertion into the α-C−H bond of **2**. The optimized geometries for both quintet and triplet states are shown in Figure 4. Structure **3** (^{5}A″) is 34.3 kcal/mol above **1** (^{5}A″) and is a true local minimum on the potential energy surface. Shown in Figure 4, **3** (^{5}A″), a C_1

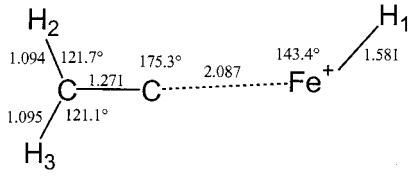

4a (^{5}A", C_s)

Figure 5. Optimized geometries of the quintet state of $HFe(CCH_2)^+$ (bond lengths in Å and bond angles in deg).

symmetry structure by calculation, is in fact a slightly distorted C_{2v} structure. In comparison to **2** (^{5}A″), the Fe−H bond is increased significantly, from 1.575 to 1.989 Å. The C−C bond distance of 1.223 Å indicates a C−C triple bond. The Fe−C bond length is 1.860 Å, which is 0.063 Å shorter than that in **1** (^{5}A″). Interestingly, the two hydrogen atoms are located very close to each other, as indicated by a small H−Fe−H bond angle of 22.2°. The H−H distance is only 0.765 Å, which is only slightly greater than the H−H bond length (0.743 Å) in a free H_2 molecule. These structural features are indicative of an H_2 molecule bound to the metal.[38−41] **3** (^{3}A″) is found to be 20.5 kcal/mol less stable than **3** (^{5}A″). It also has C_1 symmetry and displays structural features similar to those described for **3** (^{5}A″).

5. $HFe(CCH_2)^+$. $HFe(CCH_2)^+$, **4**, can be generated by the tautomerization of the acetylene complex **2**. This acetylene−vinylidene rearrangement is an important process which occurs during the reaction course of transition-metal-catalyzed processes of alkynes.[42−44] Recently, Stegmann and Frenking[45] studied the mechanism for the rearrangement of the acetylene complex $[F_4W(CHCH)]$ (**A**) to the vinylidene isomer $[F_4W(CCH_2)]$ (**B**) by theory. The acetylene complex **A** is only 10.4 kcal/mol lower in energy than the isomeric vinylidene complex **B**; however, the direct 1,2-hydrogen migration involves a barrier of 84.8 kcal/mol with respect to **A**.

Only the quintet state of **4** is located on the potential energy surface. The optimized geometry of **4** (^{5}A″) is shown in Figure 5 and has C_s symmetry. **4** (^{5}A″) is less stable than **2** (^{5}A″) by 19.4 kcal/mol and is a true local minimum. The Fe−H bond length is 1.581 Å, which is only slightly longer than that in **2** (^{5}A″, 1.575 Å). The Fe−H bond is bending toward one side, resulting in an H_1−Fe−C bond angle of 143.4°. The vinylidene unit in the complex is only slightly distorted compared to free vinylidene.[46] The C−C bond length of 1.271 Å falls between 1.208 Å (a C−C triple bond) in **2** (^{5}A″) and 1.331 (a C−C double bond) Å in **1** (^{5}A″). The Fe−C−C bond angle is 175.3°. An Fe−C distance of 2.087 Å is observed in **4** (^{5}A″) and is 0.164 Å longer than the Fe−C single-bond length in **1** (^{5}A″) and 0.227 Å longer than that in **3** (^{5}A″), which seems inconsistent with the expected Fe−C double bond. However, these structural features may suggest a loose ion−dipole interaction between FeH^+ and the CCH_2 unit. Attempts to optimize the geometry of the triplet state of **4** were not successful. The targeted structure simply collapsed to a vinyl structure.

Table 1. Pseudo-First-Order Rate Constants and Calculated Reaction Efficiencies

reacn	k_L[a]	$10^{10}k_{obsd}$[a]	eff[b] (%)
$FeH^+ + C_2D_2 \rightarrow FeD^+ + C_2HD$	9.9×10^{-10}	2.3	23
$FeD^+ + C_2H_2 \rightarrow FeH^+ + C_2HD$	1.0×10^{-9}	2.9	29
$FeH^+ + C_2D_4 \rightarrow FeD^+ + C_2HD_3$	1.0×10^{-9}	2.5	25
$FeD^+ + C_2H_4 \rightarrow FeH^+ + C_2H_3D$	1.1×10^{-9}	4.8	44
$FeC_4H_5^+ + C_2H_2 \rightarrow FeH^+ + C_6H_6$	9.3×10^{-10}	5.2	56
$FeC_2H_3^+ + C_2H_2 \rightarrow FeC_2H^+ + C_2H_4$	9.6×10^{-10}	3.8	40

[a] In units of cm^3 $molecule^{-1}$ s^{-1}. [b] Efficiency.

Experimental Studies. 1. $[Fe, C_2, H_3]^+$ System. $FeC_2H_3^+$ ions proved to be challenging to generate in the gas phase. There is no direct precursor organometallic species from which simple electron ionization would yield the desired ion. Consequently, we attempted to generate this ion *in situ* by ion−molecule reactions. Several different synthetic approaches were tried before we found a successful way of producing $FeC_2H_3^+$ cations. $FeCH_3^+$, generated by reacting Fe^+ with CH_3I, reacts with propyne to yield $FeC_2H_3^+$ (reaction 4).[47] However,

$$FeCH_3^+ + CH_3CCH \rightarrow FeC_2H_3^+ + C_2H_4 \qquad (4)$$

the intensity of $FeC_2H_3^+$ was too low for further experimental studies. Another approach involves the direct reaction of FeH^+ with C_2H_2 to form an adduct. FeH^+ was prepared from CID or SORI-CID on protonated iron pentacarbonyl, $HFe(CO)_5^+$, generated by CI with CH_5^+. Not surprisingly, no adduct was generated. Instead, reaction of FeH^+ with C_2D_2 results in H/D exchange to form FeD^+ (reaction 5). Similarly, reaction of FeD^+ and C_2H_2 yields H/D exchange (reaction 6), however, at a relatively higher exchange rate than reaction 5. The rate constants for reactions 5 and 6 are

$$FeH^+ + C_2D_2 \rightarrow FeD^+ + C_2HD \qquad (5)$$

$$FeD^+ + C_2H_2 \rightarrow FeH^+ + C_2HD \qquad (6)$$

2.3×10^{-10} cm^3 $molecule^{-1}$ s^{-1} (efficiency 23%) and 2.9×10^{-10} cm^3 $molecule^{-1}$ s^{-1} (efficiency 29%), respectively (Table 1). Although no $FeC_2H_3^+$ is formed, the H/D exchange reactions strongly suggest the formation of $Fe(CHCH_2)^+$ as a short-lived intermediate. We also tried to generate $FeC_2H_3^+$ by reaction of FeH^+ with vinyl halides, $CH_2{=}CHX$ (X = Br, Cl). However, no $FeC_2H_3^+$ was produced. Instead, FeX^+ is formed with loss of C_2H_4 (reaction 7). Although this strategy failed to give the

$$FeH^+ + CH_2CHX \rightarrow FeX^+ + C_2H_4 \qquad (7)$$

$$\not\rightarrow FeC_2H_3^+ + HX$$

(38) Kubas, G. J.; Ryan, R. R. *Polyhedron* **1986**, *5*, 473.
(39) Morris, R. H.; Sawyer, J. F.; Shiralian, M.; Zubkowski, J. D. *J. Am. Chem. Soc.* **1985**, *107*, 5581.
(40) Ricci, J. S.; Koetzle, T. F.; Bautista, M. T.; Hofstede, T. M.; Morris, R. H.; Sawyer, J. F. *J. Am. Chem. Soc.* **1989**, *111*, 8823.
(41) Van Der Sluys, L. S.; Eckert, J.; Eisenstein, O.; Hall, J. H.; Huffman, J. C.; Jackson, S. A.; Koetzle, T. F.; Kubas, G. J.; Vergamini, P. J.; Caulton, K. G. *J. Am. Chem. Soc.* **1990**, *112*, 4831.
(42) Bianchini, C.; Peruzzini, M.; Zanobini, F.; Frediani, P.; Albinati, A. *J. Am. Chem. Soc.* **1991**, *113*, 5453.
(43) Wakatsuki, Y.; Yamazaki, H.; Kumegawa, N.; Satoh, T.; Satoh, J. Y. *J. Am. Chem. Soc.* **1991**, *113*, 9604.
(44) Trost, B. M.; Dyker, G.; Kulawiec, R. J. *J. Am. Chem. Soc.* **1992**, *114*, 5476.
(45) Stegmann, R.; Frenking, G. *Organometallics* **1998**, *17*, 2089.
(46) Gallo, M. M.; Hamilton, T. P.; Schaefer, H. F., III. *J. Am. Chem. Soc.* **1990**, *112*, 8714.
(47) Jacobson, D. B.; Freiser, B. S. *J. Am. Chem. Soc.* **1985**, *107*, 5876.

desired $FeC_2H_3^+$ cation, a similar approach turns out to be ideal for producing the related $FeC_2H_5^+$ cation. FeH^+ and CH_3CH_2Cl react to form two major product ions, $FeCl^+$ and $FeC_2H_5^+$ (reactions 8 and 9). The

$$FeH^+ + CH_3CH_2Cl \xrightarrow{45\%} FeCl^+ + C_2H_6 \quad (8)$$

$$\xrightarrow{55\%} FeC_2H_5^+ + HCl \quad (9)$$

$FeC_2H_5^+$ ions can be easily isolated to allow for further studies. Schwarz and co-workers studied the $FeC_2H_5^+$ ion in an ion beam instrument; however, they were unable to generate it in their FTICR instrument.[9]

Our final and successful approach allows us to form sufficient amounts of $FeC_2H_3^+$ ions. This approach involved a multistep procedure which takes advantage of the unique features of FTICR. Acetylene is leaked into the cell at a static pressure of 1.1×10^{-7} Torr with methane added to a total pressure of 3.3×10^{-6} Torr. Methane serves both as a chemical ionization reagent and as the collision gas for CID experiments. $Fe(CO)_5$ is introduced into the vacuum chamber via a General Valve Series 9 pulsed solenoid valve. Protonated iron pentacarbonyl ($HFe(CO)_5^+$), generated by CI with CH_5^+, is first isolated. No reaction was observed between $HFe(CO)_5^+$ and C_2H_2; however, C_2H_2 readily displaces CO from $HFe(CO)_x^+$ ions ($x = 1-4$). Sequential SORI-CID on $HFe(CO)_5^+$ ions results in loss of CO molecules (reaction 10). The subsequent fragment ions $HFe(CO)_x^+$

$$HFe(CO)_5^+ \xrightarrow{SORI} HFe(CO)_4^+ \xrightarrow{SORI} HFe(CO)_3^+ \xrightarrow{SORI} HFe(CO)_2^+ \xrightarrow{SORI} HFe(CO)^+ \quad (10)$$

($x = 1-4$) undergo rapid ligand displacement with C_2H_2 (reaction 11). The desired $FeC_2H_3^+$ ion can be obtained by CID or SORI-CID on the ligand exchange products, $HFe(C_2H_2)(CO)_x^+$ ($x = 1-3$) (reaction 12).

$$HFe(CO)_x^+ + C_2H_2 \rightarrow HFe(C_2H_2)(CO)_{x-1}^+ + CO \quad (11)$$

$$HFe(C_2H_2)(CO)_x^+ \xrightarrow[SORI]{CID\ or} FeC_2H_3^+ + xCO \quad (12)$$

The CID and SORI-CID breakdown curves for $FeC_2H_3^+$ are shown in Figures 6 and 7, respectively. FeH^+ and Fe^+, corresponding to C_2H_2 and C_2H_3 losses, are the only two fragments observed. Under CID conditions, the fragment ion, FeH^+, dominates at low collision energies, while Fe^+ dominates at high collision energies. Fe^+ could come directly from Fe−C bond cleavage of $Fe(CHCH_2)^+$, as well as from consecutive fragmentations (i.e., C_2H_2 and H losses). In the low-energy SORI-CID plot, loss of C_2H_2 to form FeH^+ dominates over the whole energy range studied, indicating that loss of the C_2H_2 unit is the lowest energy decomposition pathway.

Now we take a closer look at the potential energy surface (Figure 8). Presumably, the $[Fe, C_2, H_3]^+$ ion, synthesized in reaction 12, corresponds to structure **1**, the global minimum on the potential energy surface. On the quintet surface, the activation barrier for **1** → **2** conversion is 36.8 kcal/mol with respect to **1**. For high-energy CID, the large amount of internal energy acquired from the collisional activation process can easily overcome this barrier of 36.8 kcal/mol that leads to

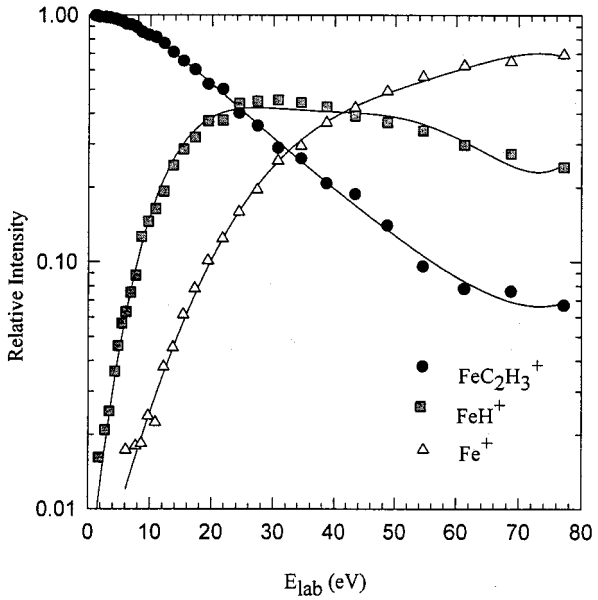

Figure 6. Energy-resolved CID breakdown curve of $FeC_2H_3^+$.

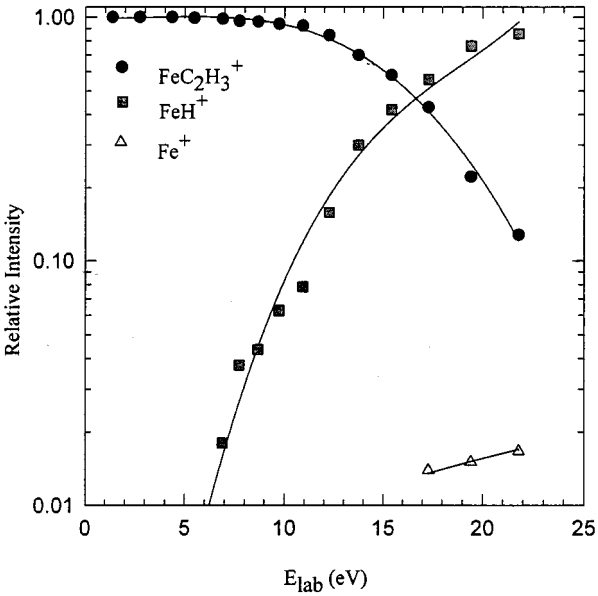

Figure 7. Energy-resolved SORI-CID breakdown curve of $FeC_2H_3^+$.

rearrangement to structure **2** and subsequent decomposition to form FeH^+ and C_2H_2. It can also lead to direct dissociation of $Fe(CHCH_2)^+$ to yield Fe^+ and C_2H_3, a process requiring 71.7 kcal/mol estimated by calculations. SORI-CID, which results in sequential activation of ions by transferring only small increments of internal energy, facilitates low-energy rearrangements prior to decomposition. Therefore, along the reaction coordinate, **1** → **2** conversion is energetically accessible since **1** can be gradually activated to overcome this barrier and rearrange to **2**. With excess internal energy, structure **2** would then decompose to yield FeH^+.

As mentioned above, there is no observable reaction between FeH^+ and C_2H_2. The activation barrier for **2** → **1** conversion is only 18.3 kcal/mol with respect to **2**. Bringing FeH^+ and C_2H_2 together will leave **2** with ca. 33 kcal/mol excess internal energy, which can easily overcome this 18.3 kcal/mol activation barrier to re-

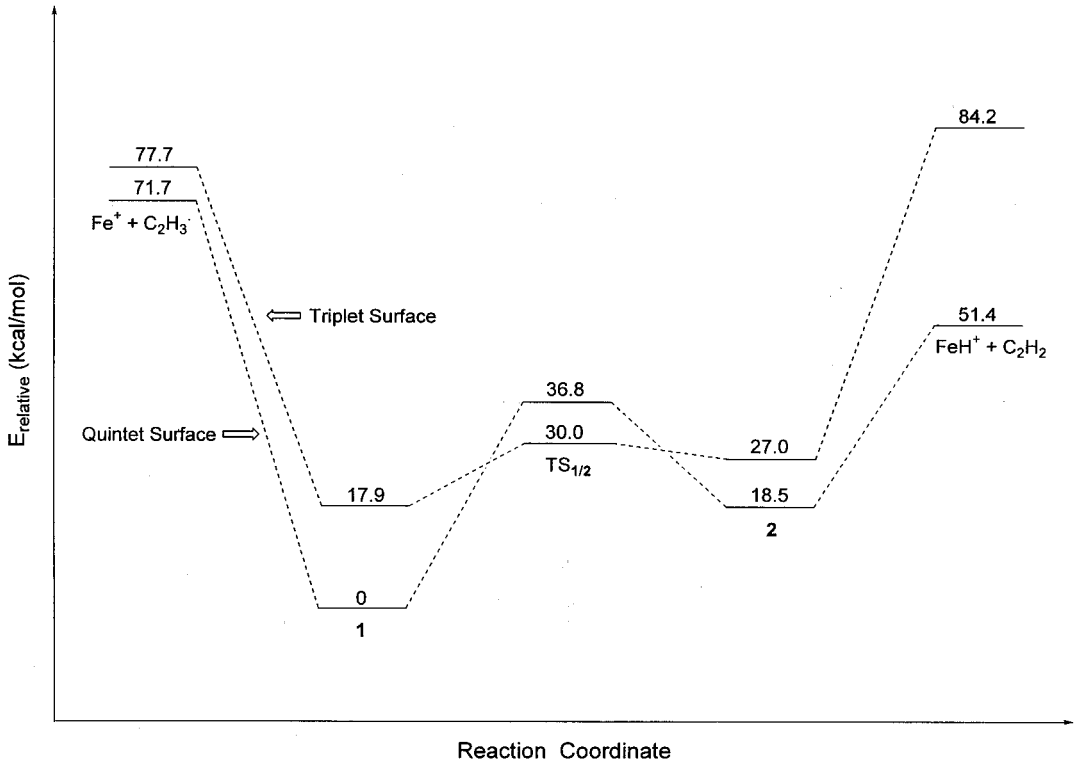

Figure 8. Potential energy surface diagram of the [Fe, C_2, H_3]$^+$ system.

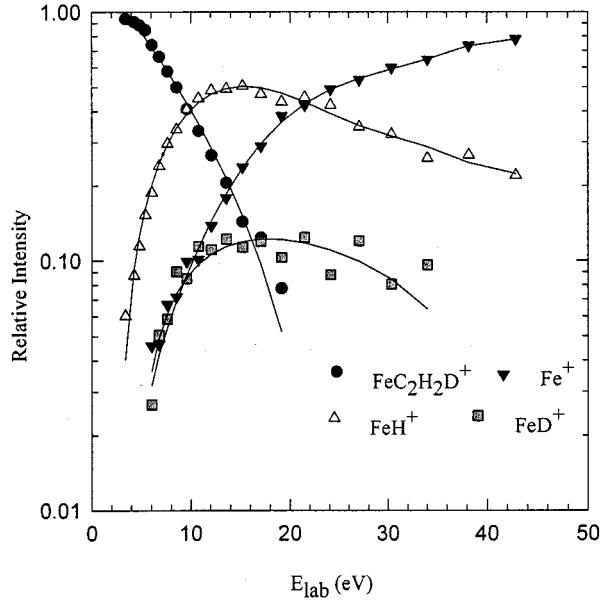

Figure 9. Energy-resolved CID breakdown curve of $FeC_2H_2D^+$.

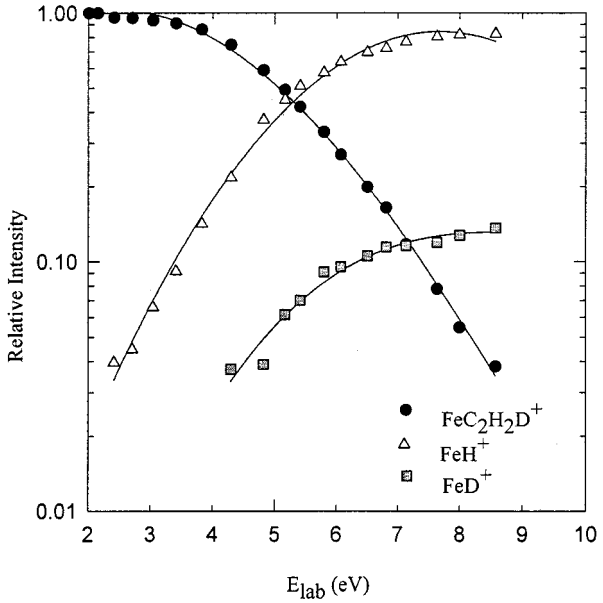

Figure 10. Energy-resolved SORI-CID breakdown curve of $FeC_2H_2D^+$.

arrange to **1**. Again, **1** → **2** conversion would also be occurring at the same time, provided that the total internal energy is preserved in the system. If this is the case, we would expect that the facile **1** ↔ **2** interconversion occurring before dissociation would result in rapid H/D exchanges (reactions 5 and 6). Indeed, reactions 5 and 6 take place at 23% and 29% of the collision rate, respectively. Isotopic labeling of $FeC_2H_3^+$, for example (reaction 13), results in the generation of

$$DFe(CO)^+ + C_2H_2 \rightarrow FeC_2H_2D^+ + CO \quad (13)$$

$FeC_2H_2D^+$. The CID and SORI-CID breakdown curves for $FeC_2H_2D^+$ are illustrated in Figures 9 and 10, respectively. CID of $FeC_2H_2D^+$ yields FeH^+ (C_2HD loss), FeD^+ (C_2H_2 loss), and Fe^+ (reactions 14−16). The ratio

$$FeC_2H_2D^+ \xrightarrow{CID} \begin{cases} FeH^+ + C_2HD & (14) \\ FeD^+ + C_2H_2 & (15) \\ Fe^+ + (C_2H_2D) & (16) \end{cases}$$

of FeH^+ to FeD^+ is 4.3:1 for CID and 6.6:1 for SORI-CID. Random H/D scrambling prior to dissociation would yield an FeH^+:FeD^+ ratio of 2:1. Upon SORI-CID,

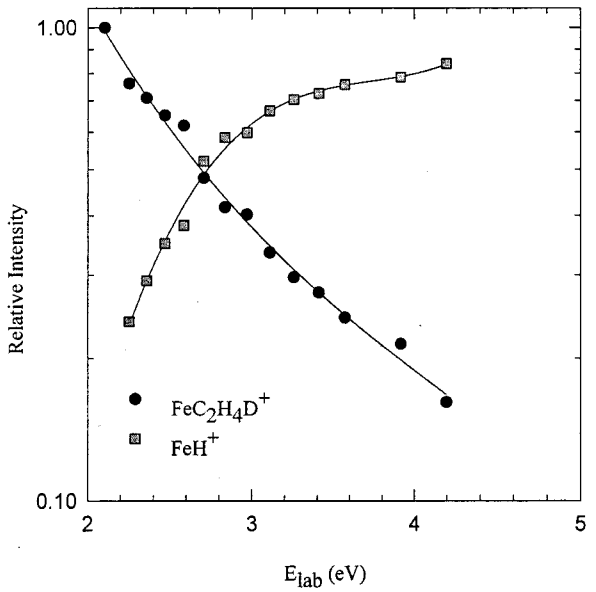

Figure 11. Energy-resolved SORI-CID breakdown curve of $FeC_2H_4D^+$.

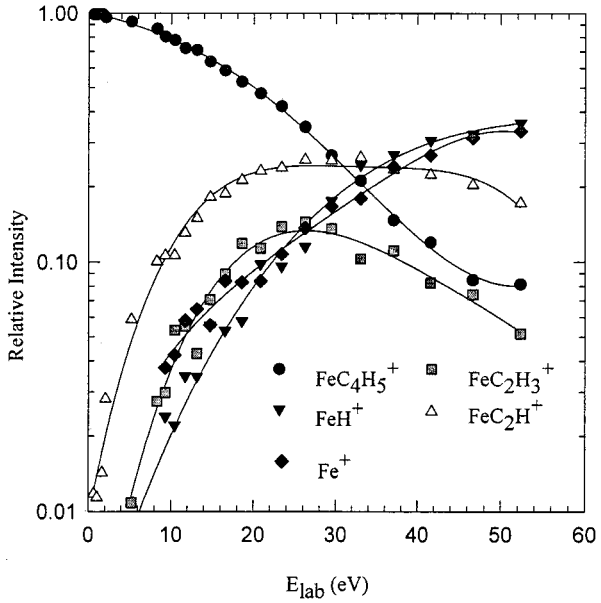

Figure 12. Energy-resolved CID breakdown curve of $FeC_4H_5^+$.

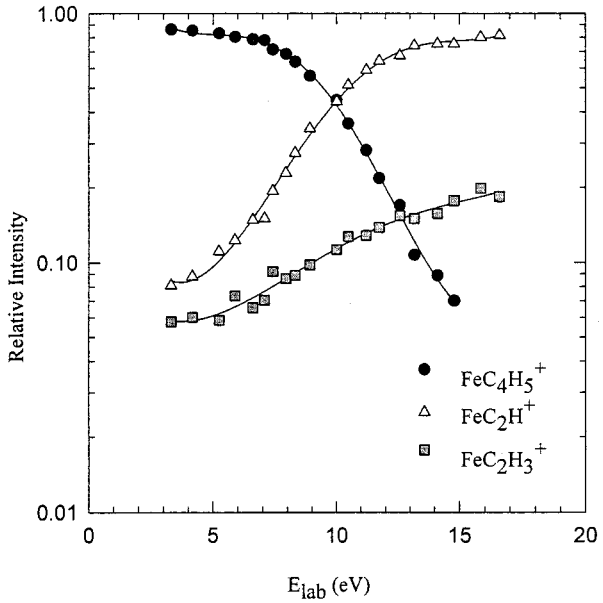

Figure 13. Energy-resolved SORI-CID breakdown curve of $FeC_4H_5^+$.

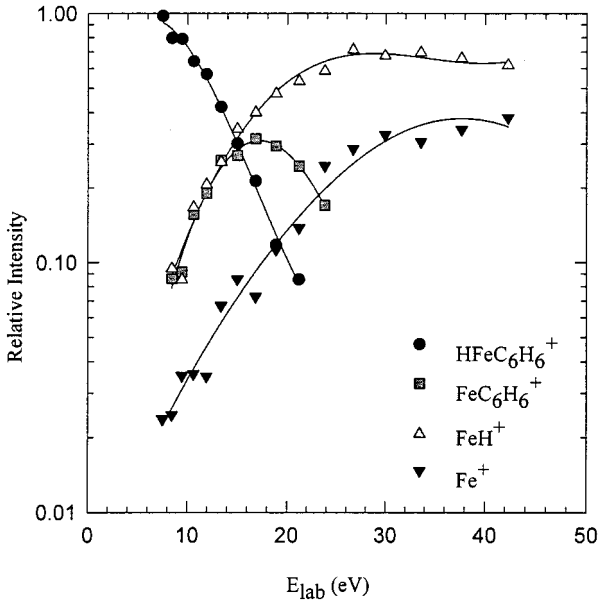

Figure 14. Energy-resolved CID breakdown curve of $HFe(C_6H_6)^+$.

1 and **2** freely interconvert prior to dissociation; however, the deuterium clearly prefers to remain on the acetylene ligand. This result can be explained by kinetic isotope effects[48] in which the deuterium prefers to be bound to the acetylene unit over Fe due to the stronger C−D bond. The H/D exchange kinetics (reactions 5 and 6) are also consistent with this kinetic isotope effect.

On the basis of the results from the H/D exchange reactions and isotopic labeling experiments, we conclude that **1** ↔ **2** interconversion is facile upon activation of **1**. Indeed, $TS_{1/2}$ is situated well below the two fragmentation channels leading to Fe^+ and FeH^+, respectively.

$TS_{1/2}$ ($^3A''$) is 6.8 kcal/mol lower than $TS_{1/2}$ ($^5A''$). Consequently, it is possible that the triplet surface plays a role in the **1** ↔ **2** interconversion. However, this curve crossing is not required to explain our isotopic exchange results. We believe that the triplet surface plays little or no role in the **1** ↔ **2** interconversion.

2. [Fe, C_2, H_5]$^+$ System. [Fe, C_2, H_5]$^+$ has been synthesized and studied thoroughly by Schwarz and coworkers. As described in ref 5, adduct formation of FeH^+ with ethylene does not take place. However, H/D exchange processes turn out to be efficient (reaction 17, $k = 2.5 \times 10^{-10}$ cm^3 molecule^{-1} s^{-1}, efficiency 25%; reaction 18, $k = 4.8 \times 10^{-10}$ cm^3 molecule^{-1} s^{-1}, efficiency 44%). These results suggest formation of

$$FeH^+ + C_2D_4 \rightarrow FeD^+ + C_2HD_3 \qquad (17)$$

$$FeD^+ + C_2H_4 \rightarrow FeH^+ + C_2H_3D \qquad (18)$$

$Fe(C_2HD_4)^+/Fe(C_2H_4D)^+$ as short-lived reaction intermediates. Reaction 18 is slightly more efficient than

(48) Bullock, R. M. In *Transition Metal Hydrides*; Dedieu, A., Eds.; VCH: New York, 1992; p 263.

Scheme 1

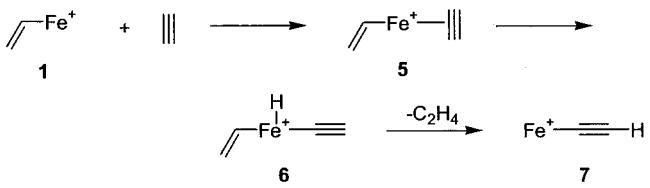

reaction 17, indicating a kinetic isotope effect similar to that for reactions 5 and 6. If the deuterium-labeled species such as $FeC_2H_4D^+$ could be generated, CID or SORI-CID of $FeC_2H_4D^+$ to induce fragmentation should yield a kinetic isotope effect similar to that observed for the $FeC_2H_2D^+$ system (*vide supra*).

As mentioned above, FeH^+ reacts with C_2H_5Cl ($k = 2.8 \times 10^{-10}$ cm^3 molecule^{-1} s^{-1}, efficiency 15%) to yield 55% of $FeC_2H_5^+$ (reaction 9) in addition to 45% of $FeCl^+$ (reaction 8). Interestingly, FeD^+ reacts with C_2H_5Cl to generate 45% of $FeCl^+$ (reaction 19) and 55% of $FeC_2H_4D^+$ (no $FeC_2H_5^+$ is observed) (reaction 20). CID of $FeC_2H_4D^+$ only yields FeH^+ (no FeD^+) at low kinetic energy (reaction 21), and the formation of Fe^+ starts to dominate at high kinetic energies (reaction 22). SORI-

$$FeD^+ + CH_3CH_2Cl \xrightarrow{45\%} FeCl^+ + C_2H_5D \quad (19)$$

$$\xrightarrow{55\%} FeC_2H_4D^+ + HCl \quad (20)$$

$$FeC_2H_4D^+ \xrightarrow{CID} FeH^+ + C_2H_3D \quad (21)$$

$$\rightarrow Fe^+ + (C_2H_4D) \quad (22)$$

CID, the low-energy fragmentation probe, yields exclusively FeH^+ (Figure 11). These results point to a dramatic kinetic isotope effect for this system. The [Fe, C_2, H_3]$^+$ system has a smaller kinetic isotope effect, as described earlier.

3. Reaction of $FeC_2H_3^+$ with C_2H_2. Interestingly, when $FeC_2H_3^+$ is trapped in the FTICR cell with C_2H_2, reaction 23 occurs. Density functional calculations

$$FeC_2H_3^+ + C_2H_2 \rightarrow FeC_2H^+ + C_2H_4 \quad (23)$$

predict ΔH, the heat of reaction, to be only −3 kcal/mol, indicating a slightly exothermic reaction. Listed in Table 1, the rate constant for reaction 23 is 3.8×10^{-10} cm^3 molecule^{-1} s^{-1} (40% efficiency). CID of FeC_2H^+ yields Fe^+ exclusively.

The initial step in the reaction possibly involves formation of the collision complex **5** with insertion into the acetylenic C−H bond to yield **6** followed by ethene reductive elimination to yield **7** (Scheme 1). To further investigate this reaction, the collision complex with elemental composition [Fe, C_4, H_5]$^+$ is formed by CID or SORI-CID of $HFe(C_2H_2)_2(CO)_x^+$ ($x = 1-3$) (reaction 24), which comes from multiple ligand exchange of CO

$$HFe(C_2H_2)_2(CO)_x^+ \xrightarrow[SORI]{CID\ or} FeC_4H_5^+ + xCO \quad (24)$$

by C_2H_2. CID and SORI-CID breakdown curves of $FeC_4H_5^+$ are shown in Figures 12 and 13, respectively. Two competitive fragmentation channels are observed, namely simple cleavage of C_2H_2 (reaction 25) and rearrangement to form **7,** FeC_2H^+, with loss of C_2H_4

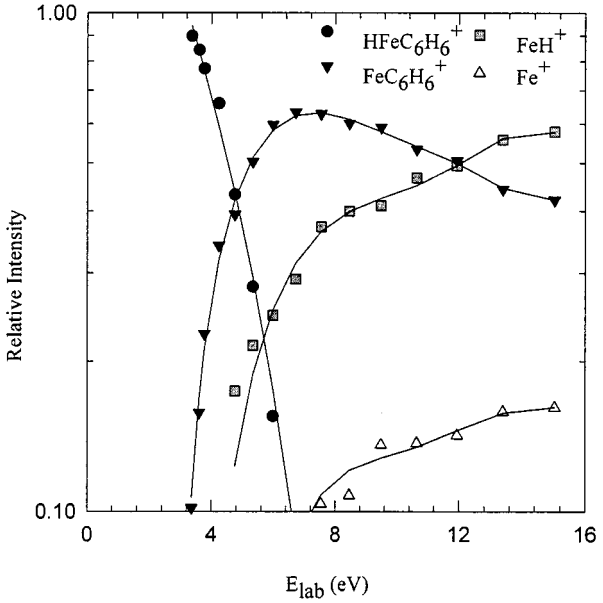

Figure 15. Energy-resolved SORI-CID breakdown curve of $HFe(C_6H_6)^+$.

(reaction 26). The structure of $FeC_4H_5^+$ could be either

$$FeC_4H_5^+ \xrightarrow[SORI]{CID\ or} FeC_2H_3^+ + C_2H_2 \quad (25)$$

$$\rightarrow FeC_2H^+ + C_2H_4 \quad (26)$$

5 or **8**. SORI-CID results indicate that loss of C_2H_4 to yield **7** is the lowest energy decomposition channel.

$FeC_4H_5^+$ reacts with C_2H_2 to generate FeH^+, presumably by eliminating benzene, reaction 27 ($k = 5.2 \times 10^{-10}$ cm^3 molecule^{-1} s^{-1}, efficiency 56%). Trimerization of acetylene to form benzene (reaction 28) is exothermic by 143 kcal/mol.[49] Therefore, we would expect that

$$FeC_4H_5^+ + C_2H_2 \rightarrow FeH^+ + C_6H_6 \quad (27)$$

$$3C_2H_2 \rightarrow C_6H_6 \quad (28)$$

reaction 27 is also relatively exothermic. The intermediate $HFe(C_6H_6)^+$ would, therefore, contain a large amount of excess internal energy resulting in fragmentation to yield FeH^+ and benzene. An authentic $HFe(C_6H_6)^+$ ion is generated by reacting FeH^+ with benzene. CID of $HFe(C_6H_6)^+$ (Figure 14) indicates that loss of benzene and hydrogen are competitive processes (reactions 29 and 30). Low energy SORI-CID (Figure 15) further

$$HFe(C_6H_6)^+ \xrightarrow{CID} FeH^+ + C_6H_6 \quad (29)$$

$$\rightarrow Fe(C_6H_6)^+ + H^\cdot \quad (30)$$

$$\rightarrow Fe^+ + (C_6H_7) \quad (31)$$

(49) This calculation is based on heats of formation taken from the reference: Lias, S. G.; Bartmess, J. E.; Liebman, J. F.; Holmes, J. L.; Levin, R. D.; Mallard, W. G. Gas-Phase Ion and Neutral Thermochemistry. *J. Phys. Chem. Ref. Data* **1988**, *17*, Suppl. No. 1.

suggests that loss of hydrogen to form $Fe(C_6H_6)^+$ is the lowest energy fragmentation channel.

Conclusions

Information on the geometries and energetics for the [Fe, C_2, H_3]$^+$ isomers **1**−**4** was obtained by density functional calculations. The transition state connecting **1** and **2** was also located on the potential energy surface. For example, on the quintet PES, **1** → **2** conversion essentially involves a β-hydrogen transfer with an activation barrier of 36.8 kcal/mol. *In situ* synthesis of **1** in the gas phase is achieved by a complex, multistep sequence yet yields a strong $FeC_2H_3^+$ signal. CID and SORI-CID results indicate that **1** → **2** conversion with a 36.8 kcal/mol barrier is accessible which eventually leads to subsequent fragmentation of **2**. On the other hand, H/D exchange reaction between FeH^+/FeD^+ and C_2D_2/C_2H_2 provides solid evidence for **2** → **1** conversion, a rapid process involving an activation barrier of 18.3 kcal/mol. Therefore, we conclude that **1** ↔ **2** interconversion is facile for activated **1** and **2**. Reaction of $FeC_2H_3^+$ with C_2H_2 yields exclusive formation of FeC_2H^+. CID and SORI-CID of the corresponding collision complex, $FeC_4H_5^+$, indicate that loss of C_2H_4 to yield FeC_2H^+ is the lowest energy decomposition channel. Reaction of $FeC_4H_5^+$ with C_2H_2 yields exclusive loss of benzene. In addition, H/D exchange reactions between FeH^+/FeD^+ and C_2D_4/C_2H_4 were also investigated, providing complementary information to Schwarz's studies of the [Fe, C_2, H_5]$^+$ system. Once again, the combination of experimental investigation and theoretical calculations provides a powerful means for understanding simple organo-transition-metal ion rearrangements.

Acknowledgment. This paper is dedicated to the memory of Dr. Ben S. Freiser. Acknowledgment is made to the Division of Chemical Science in the Office of Basic Energy Sciences in the United States Department of Energy (under Grant DE-FG02-87ER13766) for supporting this research.

OM9902941